Synthesis and Manipulation of High Aspect Ratio Gold Nanorods Grown Directly on Surfaces

Zhongqing Wei, Aneta J. Mieszawska, and Francis P. Zamborini*

Department of Chemistry, University of Louisville, Louisville, Kentucky 40292

Received February 3, 2004. In Final Form: March 25, 2004

Here we describe the synthesis of Au nanorods directly on glass surfaces using seed-mediated deposition of Au from $AuCl_4^-$ onto surface-attached 3−5 nm diameter Au nanoparticles (AuNPs) in the presence of cetyltrimethylammonium bromide (CTAB). The average length (200 nm to 1.2 μm) and aspect ratio (6−22) of the nanorods increases with increasing $AuCl_4^-$ concentration. Short, low aspect ratio Au nanorods are manipulated with an atomic force microscopy (AFM) tip, while longer, high aspect ratio nanorods are bent and broken with the AFM tip.

The controlled synthesis of anisotropic, one-dimensional (1D) nanostructures, such as wires, rods, belts, and tubes, has received enormous attention due to the fundamentally interesting growth mechanisms and importance in the fabrication of nanoscale devices.[1] Gold nanorods are 1D structures that have fascinating, size-dependent optical properties[2−7] and the ability to enhance surface Raman scattering[8,9] and fluorescence signals.[7,10,11] There are also reports on the thermal[12,13] and photothermal[14−19] reshaping, melting, fragmentation, and vibrational properties of Au nanorods as well as their surface structure[20−24] and diffusion[25] on functionalized surfaces. Au and Au-containing mixed-metal nanorods have been utilized for nanoscale barcode identification,[26,27] gene delivery,[28] nanoelectronics,[29,30] and template synthesis of hollow nanostructures.[31] Several procedures exist for preparing 1D Au and mixed-metal Au-containing nanomaterials, including electrochemical deposition in templates,[2,3,26−30,32] electrochemical deposition at step edges,[33−35] electrochemical synthesis,[4,14,36−38] photochemical synthesis,[39−42] microwave heating,[43,44] and seed-mediated growth.[45−53]

The seed-mediated growth of Au nanorods described by Murphy and co-workers[46−50,52,53] is an attractive method because of its simplicity and control over the nanorod aspect ratio (AR) through synthetic conditions.[46,47,49,52] The procedure involves the chemical reduction of $AuCl_4^-$ by ascorbic acid, a weak reducing agent, in the presence of

* To whom correspondence should be addressed. E-mail: f.zamborini@louisville.edu.

(1) Xia, Y.; Yang, P.; Sun, Y.; Wu, Y.; Mayers, B.; Gates, B.; Yin, Y.; Kim, F.; Yan, H. *Adv. Mater.* **2003**, *15*, 353−389.
(2) Foss, C. A.; Hornyak, G. L.; Stockert, J. A.; Martin, C. R. *J. Phys. Chem.* **1992**, *96*, 7497−7499.
(3) Foss, C. A.; Hornyak, G. L.; Stockert, J. A.; Martin, C. R. *J. Phys. Chem.* **1994**, *98*, 2963−2971.
(4) Yu, Y.-Y.; Chang, S.-S.; Lee, C.-L.; Wang, C. R. C. *J. Phys. Chem. B* **1997**, *101*, 6661−6664.
(5) Link, S.; El-Sayed, M. A. *J. Phys. Chem. B* **1999**, *130*, 8410−8426.
(6) van der Zande, B. M. I.; Boehmer, M. R.; Fokkink, L. G. J.; Schoenenberger, C. *Langmuir* **2000**, *16*, 451−458.
(7) El-Sayed, M. A. *Acc. Chem. Res.* **2001**, *34*, 257−264.
(8) Nikoobakht, B.; Wang, J.; El-Sayed, M. A. *Chem. Phys. Lett.* **2002**, *366*, 17−23.
(9) Nikoobakht, B.; El-Sayed, M. A. *J. Phys. Chem. A* **2003**, *107*, 3372−3378.
(10) Mohamed, M. B.; Volkov, V.; Link, S.; El-Sayed, M. A. *Chem. Phys. Lett.* **2000**, *317*, 517−523.
(11) Varnavski, O. P.; Mohamed, M. B.; El-Sayed, M. A. *J. Phys. Chem. B* **2003**, *107*, 3101−3104.
(12) Mohamed, M. B.; Ismail, K. Z.; Link, S.; El-Sayed, M. A. *J. Phys. Chem. B* **1998**, *102*, 9370−9374.
(13) Mohamed, M. B.; Wang, Z. L.; El-Sayed, M. A. *J. Phys. Chem. A* **1999**, *103*, 10255−10259.
(14) Chang, S.-S.; Shih, C.-W.; Chen, C.-D.; Lai, W.-C.; Wang, C. R. C. *Langmuir* **1999**, *15*, 701−709.
(15) Link, S.; Burda, C.; Mohamed, M. B.; Nikoobakht, B.; El-Sayed, M. A. *J. Phys. Chem. A* **1999**, *103*, 1165−1170.
(16) Link, S.; Burda, C.; Mohamed, M. B.; Nikoobakht, B.; El-Sayed, M. A. *Phys. Rev. B* **2000**, *61*, 6086−6090.
(17) Link, S.; Wang, Z. L.; El-Sayed, M. A. *J. Phys. Chem. B* **2000**, *104*, 7867−7870.
(18) Link, S.; El-Sayed, M. A. *J. Chem. Phys.* **2001**, *114*, 2362−2366.
(19) Hu, M.; Wang, X.; Hartland, G. V.; Mulvaney, P.; Juste, J. P.; Sader, J. E. *J. Am. Chem. Soc.* **2003**, *125*, 14925−14933.
(20) Wang, Z. L.; Mohamed, M. B.; Link, S.; El-Sayed, M. A. *Surf. Sci.* **1999**, *440*, L809−L814.
(21) Wang, Z. L.; Gao, R. P.; Nikoobakht, B.; El-Sayed, M. A. *J. Phys. Chem. B* **2000**, *104*, 5417−5420.
(22) Yacaman, M. J.; Ascencio, J. A.; Canizal, G. *Surf. Sci.* **2001**, *486*, L449−L453.
(23) Johnson, C. J.; Dujardin, E.; Davis, S. A.; Murphy, C. J.; Mann, S. *J. Mater. Chem.* **2002**, *12*, 1765−1770.
(24) Gai, P. L.; Harmer, M. A. *Nano Lett.* **2002**, *2*, 771−774.
(25) St. Angelo, S. K.; Waraksa, C. C.; Mallouk, T. E. *Adv. Mater.* **2003**, *15*, 400−402.
(26) Nicewarner-Pena, S. R.; Griffith, F. R.; Reiss, B. D.; He, L.; Pena, D. J.; Walton, I. D.; Cromer, R.; Keating, C. D.; Natan, M. J. *Science* **2001**, *294*, 137−141.
(27) Keating, C. D.; Natan, M. J. *Adv. Mater.* **2003**, *15*, 451−454.
(28) Salem, A. K.; Searson, P. C.; Leong, K. W. *Nature Mater.* **2003**, *2*, 668−671.
(29) Kovtyukhova, N. I.; Martin, B. R.; Mbindyo, J. K. N.; Smith, P. A.; Razavi, B.; Mayer, T. S.; Mallouk, T. E. *J. Phys. Chem. B* **2001**, *105*, 8762−8769.
(30) Kovtyukhova, N. I.; Mallouk, T. E. *Chem. Eur. J.* **2002**, *8*, 4354−4363.
(31) Obare, S. O.; Jana, N. R.; Murphy, C. J. *Nano Lett.* **2001**, *1*, 601−603.
(32) Wirtz, M.; Martin, B. R. *Adv. Mater.* **2003**, *15*, 455−458.
(33) Walter, E. C.; Murray, B. J.; Favier, F.; Kaltenpoth, G.; Grunze, M.; Penner, R. M. *J. Phys. Chem. B* **2002**, *106*, 11407−11411.
(34) Penner, R. M. *J. Phys. Chem. B* **2002**, *106*, 3339−3353.
(35) Walter, E. C.; Zach, M. P.; Favier, F.; Murray, B. J.; Inazu, K.; Hemminger, J. C.; Penner, R. M. *ChemPhysChem* **2003**, *4*, 131−138.
(36) Ah, C. S.; Hong, S. D.; Jang, D.-J. *J. Phys. Chem. B* **2001**, *105*, 7871−7873.
(37) Nikoobakht, B.; El-Sayed, M. A. *Langmuir* **2001**, *17*, 6368−6374.
(38) Yao, H.; Onishi, T.; Sato, S.; Kimura, K. *Chem. Lett.* **2002**, 458−459.
(39) Esumi, K.; Nawa, M.; Aihara, N.; Usui, K. *New J. Chem.* **1998**, 719−720.
(40) Leontidis, E.; Kleitou, K.; Kyprianidou-Leodidou, T.; Bekiari, V.; Lianos, P. *Langmuir* **2002**, *18*, 3659−3668.
(41) Kim, F.; Song, J. H.; Yang, P. *J. Am. Chem. Soc.* **2002**, *124*, 14316−14317.
(42) Niidome, Y.; Koji, N.; Kawasaki, H.; Yamada, S. *Chem. Commun.* **2003**, 2376−2377.
(43) Zhu, Y.-J.; Hu, X.-L. *Chem. Lett.* **2003**, *32*, 1140−1141.
(44) Liu, F.-K.; Chang, Y.-C.; Ko, F.-H.; Chu, T.-C. *Mater. Lett.* **2004**, *58*, 373−377.
(45) Brown, K. R.; Walter, D. G.; Natan, M. J. *Chem. Mater.* **2000**, *12*, 306−313.
(46) Jana, N. R.; Gearheart, L.; Murphy, C. J. *J. Phys. Chem. B* **2001**, *105*, 4065−4067.
(47) Jana, N. R.; Gearheart, L.; Murphy, C. J. *Adv. Mater.* **2001**, *13*, 1389−1393.
(48) Jana, N. R.; Gearheart, L.; Murphy, C. J. *Chem. Mater.* **2001**, *13*, 2313−2322.
(49) Murphy, C. J.; Jana, N. R. *Adv. Mater.* **2002**, *14*, 80−82.
(50) Jana, N. R.; Gearheart, L.; Obare, S. O.; Murphy, C. J. *Langmuir* **2002**, *18*, 922−927.

10.1021/la049702i CCC: $27.50
Published on Web 04/21/2004

cetyltrimethylammonium bromide (CTAB) onto preformed Au nanoparticle (AuNP) seeds in aqueous solutions. Although the details of nanorod formation are not completely understood, it is believed that the CTAB adsorbs more strongly (as a bilayer)[37] along the long axis crystal face of the Au nanorod, allowing growth to occur preferentially on the ends of the nanorod[20−24,53] as opposed to the CTAB forming a soft rodlike micellar template[54] for the rods to grow in. In solution systems, the AR of the nanorods and confinement of growth to preformed Au seeds depends on the $AuCl_4^-$/Au seed ratio.[46−49] In most cases, the yield of nanorods is rather low (4−20%) and the samples contain large size dispersity.[46,47,52] Yields are greatly improved by increasing the pH[52] or adding Ag^+ ions[51] and nanorods can be purified by centrifugation[46,47,52] or surfactant-assisted assembly.[55] With these variations, samples with >90% nanorods are prepared. The AR of Au nanorods increases by adding heptane[52] or a second type of cosurfactant (benzyldimethylammonium chloride, BDAC)[51] to the growth solution. Ag[56] and Cu[57] nanorods have also been prepared using seed-mediated growth.

Taub et al. recently described the seed-mediated growth of Au nanorods directly on mica and silicon surfaces by chemically attaching AuNP seeds to the surface and placing the substrate in a solution of $AuCl_4^-$, CTAB, and ascorbic acid.[58] In this paper we report on the seed-mediated growth of Au nanorods directly on glass surfaces using a similar procedure, except that we used a different linker to chemically attach the AuNP seeds to the surface and we varied the $AuCl_4^-$ concentration and the time in growth solution to determine their effect on the Au nanostructures. We found that the linker affects the extent of Au nucleation occurring in solution, and the average length and AR of the Au nanorods depends on $AuCl_4^-$ concentration and time. Importantly, we prepared Au nanorods >1 μm in length (AR > 20) using large $AuCl_4^-$ concentrations and growth times of 1 h in a one-step synthesis compared to the previously reported three-step procedure that produced ~500 nm long (AR = 6) Au NRs.[58] Au nanorods are also manipulated, bent, or broken with an AFM tip, depending on the AR.

Growth of Au Nanorods on Glass. Nanorods were grown directly on Corning cut glass microscope slides as shown in Scheme 1. First, the glass was functionalized by heating for 30 min in a solution containing 10 mL of 2-propanol, 100 μL of mercaptopropyltrimethoxysilane (MPTMS), and 5 to 6 drops of Nanopure water. Glass/MPTMS substrates were then placed directly in an aqueous solution of 3−5 nm AuNP seed[46] for 20 min. The functionalized glass/MPTMS/AuNP slide was removed, rinsed with water, and placed in a nanorod growth solution at 25 °C for either 1 or 21 h as indicated. The nanorod growth solution was comprised of 9.0 mL of 0.1 M CTAB plus 22, 112, 225, 450, or 675 μL of 0.01 M $HAuCl_4 \cdot 3H_2O$ (as indicated) plus 0.05 or 0.10 mL of 0.1 M ascorbic acid,[59] added in that order.

Scheme 1. Procedure for Growing High Aspect Ratio Surface-Attached Au Nanorods

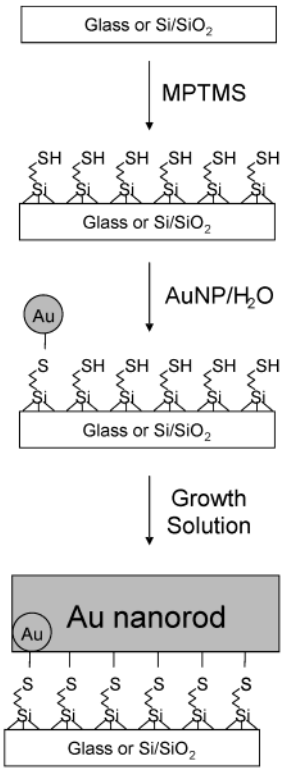

The glass/MPTMS/AuNP slide turned from colorless to pink after being placed in growth solution due to the deposition of Au on the surface. The growth solution remained colorless, indicating that no, or very little, nucleation of Au occurs in the growth solution under these conditions (Figure S1, Supporting Information). When (aminopropyl)triethoxysilane (APTES) was used to link AuNPs to the surface, we observed two main differences. First, the glass slide turned pink following immersion in AuNP seed for 20 min due to higher coverage of seed particles on the surface (Figure S2, Supporting Information). Second, when the slide was subsequently placed in growth solution, the growth solution turned a very noticeable pink/purple color, indicating that substantial nucleation of Au occurs in solution instead of being confined to the surface only (Figure S1, Supporting Information). MPTMS was used exclusively as a linker in these studies to prevent the nucleation of Au in solution. As shown in Scheme 1, the nanorods are presumably attached through Au−thiolate bonds, but there is no direct evidence of the surface interactions.

Microscopy. A Veeco Metrology Multimode Nanoscope IIIA atomic force microscope (AFM) operating in tapping mode was employed to characterize the size and shape of the surface-grown Au nanostructures. Frames A−D of Figure 1 show representative AFM images of four glass/MPTMS/AuNP samples after they were placed in four different growth solutions for 1 h that contained 112, 225, 450, and 675 μL of $AuCl_4^-$, respectively. Au nanorods are observed in all images along with other shapes, such as nanoparticles, triangles, and hexagons. The size of the nanostructures increases with increasing amounts of $AuCl_4^-$, but more importantly, the length, AR, and number of Au nanorods increases with increasing $AuCl_4^-$ concentration. The average lengths and AR observed for

(51) Nikoobakht, B.; El-Sayed, M. A. *Chem. Mater.* **2003**, *15*, 1957−1962.
(52) Busbee, B. D.; Obare, S. O.; Murphy, C. J. *Adv. Mater.* **2003**, *15*, 414.
(53) Gao, J.; Bender, C. M.; Murphy, C. J. *Langmuir* **2003**, *19*, 9065−9070.
(54) Tornblom, M.; Henriksson, U. *J. Phys. Chem. B* **1997**, *101*, 6028−6035.
(55) Jana, N. R. *Chem. Commun.* **2003**, 1950−1951.
(56) Jana, N. R.; Gearheart, L.; Murphy, C. J. *Chem. Commun.* **2001**, 617−618.
(57) Liu, C. M.; Guo, L.; Xu, H. B.; Wu, Z. Y.; Weber, J. *Microelectron. Eng.* **2003**, *66*, 107−114.
(58) Taub, N.; Krichevski, O.; Markovich, G. *J. Phys. Chem. B* **2003**, *107*, 11579−11582.

(59) 0.1 mL of ascorbic acid was added when 675 μL of $AuCl_4^-$ was used.

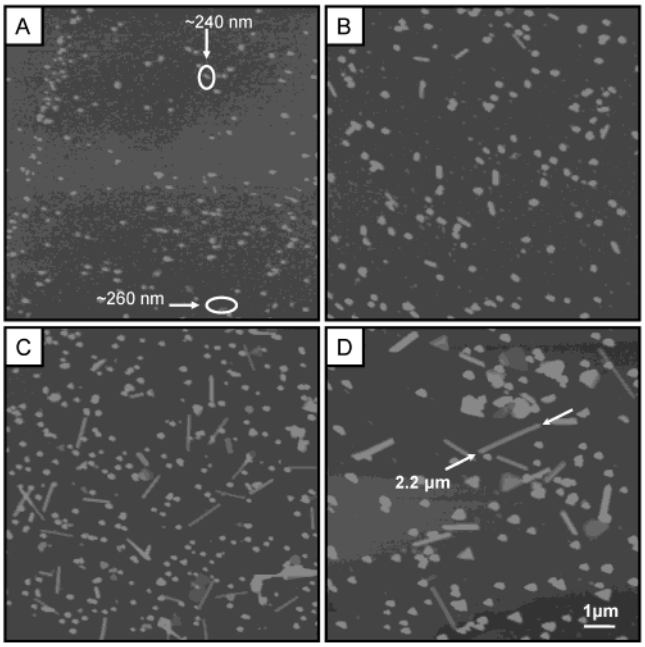

Figure 1. Atomic force microscopy (AFM) images of Au nanostructures grown by placing glass/MPTMS/AuNP samples for 1 h in a growth solution containing 9 mL of 0.1 M CTAB, 0.05 mL or 0.1 mL[59] of 0.1 M ascorbic acid, and (A) 112 μL, (B) 225 μL, (C) 450 μL, and (D) 675 μL of 0.01 M $HAuCl_4$. The scan size is 10 μm and the *z*-scale is 100 nm in all images.

nanorods in Figure 1 are 252 ± 23 nm (AR = 6.1 ± 1.8), 484 ± 103 nm (AR = 7.0 ± 3.2), 906 ± 232 nm (AR = 22.2 ± 9.3), and 1.2 ± 0.4 μm (AR = 19.7 ± 12.2) for frames A−D, respectively. Figure 1D also shows an example of a nanorod as long as 2.2 μm (AR = 50, indicated by the arrow). Clearly the size and shape of the nanostructures depends on the amount of $AuCl_4^-$ in growth solution if all other conditions are equal.

Frames A−D of Figure 2 show representative AFM images of four glass/MPTMS/AuNP samples after they were placed in four different growth solutions for 21 h that contained 22, 112, 225, and 450 μL of $AuCl_4^-$, respectively. This was performed to determine if low $AuCl_4^-$ concentrations would eventually produce long nanorods at longer times. The amount of Au present on the sample increases with increasing time in growth solution when $AuCl_4^-$ concentration is constant (compare Figure 2C with Figure 1B). Also, as in Figure 1, the size of all nanostructures increases with increasing amounts of $AuCl_4^-$ and longer, higher AR nanorods form in solutions containing higher concentrations of $AuCl_4^-$. Figure 2 (frames A−C) confirms that, with low $AuCl_4^-$ concentration, increasing the time in growth solution does not lead to the formation of long, high AR nanorods. The average lengths and AR observed for nanorods in Figure 2 are 235 ± 47 nm (AR = 3.9 ± 1.6), 384 ± 115 nm (AR = 5.2 ± 2.2), and 838 ± 365 nm (AR = 7.8 ± 4.1) for frames B−D, respectively. No nanorods are present in the sample grown from 22 μL of $AuCl_4^-$ (Frame A). It is interesting that the length of the Au nanorods does not significantly change comparing 1 h samples and 21 h samples at large $AuCl_4^-$ concentrations, but the AR changes dramatically. For example, the average length of Au nanorods prepared from 450 μL of $AuCl_4^-$ at 1 and 21 h is 906 ± 232 nm and 838 ± 365 nm, respectively, while the AR is 22.2 ± 9.3 and 7.8 ± 4.1, respectively. This implies that under these conditions, Au nanorod growth along its long axis reaches a maximum within 1 h and the nanorods then grow wider at longer times.

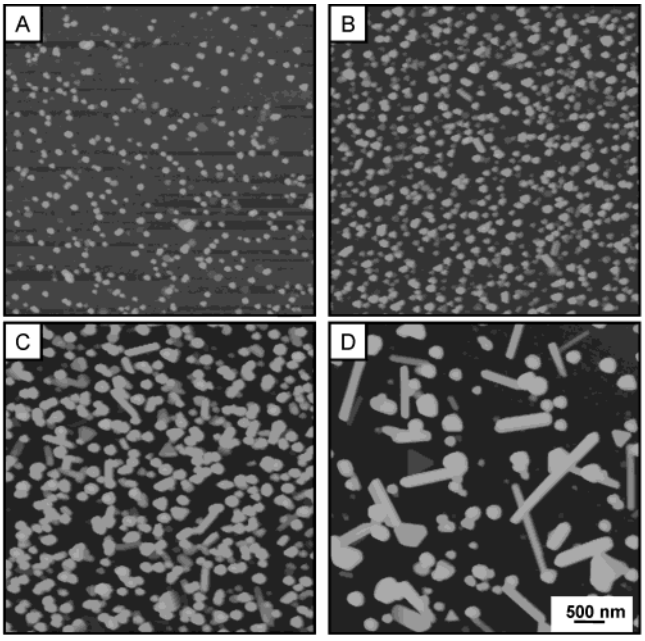

Figure 2. Atomic force microscopy (AFM) images of Au nanostructures grown by placing glass/MPTMS/AuNP samples for 21 h in a growth solution containing 9 mL of 0.1 M CTAB, 0.05 mL of 0.1 M ascorbic acid, and (A) 22 μL, (B) 112 μL, (C) 225 μL, and (D) 450 μL of 0.01 M $HAuCl_4$. The scan size is 5 μm, and the *z*-scale is 250 nm in all images.

The average lengths and AR of the nanorods discussed in the representative images of Figures 1 and 2 vary from sample-to-sample and even within the same sample, but the general trend was observed in 5 trials of the same experiment. The yield of nanorods in Figures 1 and 2 ranges from 4 to 14%, which is consistent with solution-phase and previous surface-grown nanorods.[46,52,58]

UV−vis Characterization. Figure 3 shows the UV−vis spectra of glass/MPTMS and glass/MPTMS/AuNP samples after they were placed in growth solutions containing varied amounts of $AuCl_4^-$ for 1 h (A) and 21 h (B), respectively. The absorbance of the glass/MPTMS/AuNP samples throughout the entire wavelength range increases with increasing amounts of $AuCl_4^-$ added to the growth solution for both 1 and 21 h times. The absorbance also increases with increasing time in growth solution when comparing samples containing the same amount of $AuCl_4^-$. For example, the absorbance at 300 nm of samples prepared from 225 μL of $AuCl_4^-$ increased from 0.04 at 1 h to 0.27 at 21 h. These results indicate that the amount of Au deposited on the surface increases with increasing $AuCl_4^-$ concentration or increasing time in growth solution, consistent with the AFM images. The lack of absorbance on the glass/MPTMS control slides confirms that the AuNPs act as nucleation sites or as a catalyst for Au deposition and formation of larger nanostructures. The spectra of the seeded surfaces in frames A and B of Figure 1 all exhibit a broad peak at ~520 nm, characteristic of the transverse surface plasmon band for Au nanoparticles or nanorods larger than 2.0 nm in diameter. Unfortunately, we did not observe a longitudinal plasmon band at higher wavelengths characteristic of Au nanorods. This is most likely because of the very low yield of nanorods on the surface and higher AR rods would exhibit this band outside of the wavelengths measured.[46,47,51] Au nanorods with AR > 6 exhibit a longitudinal band above 1000 nm.[51] Therefore, while the UV−vis data are useful to qualitatively show the growth of Au nanostructures on the surface, they are not useful for characterizing the presence or dimensions of Au nanorods.

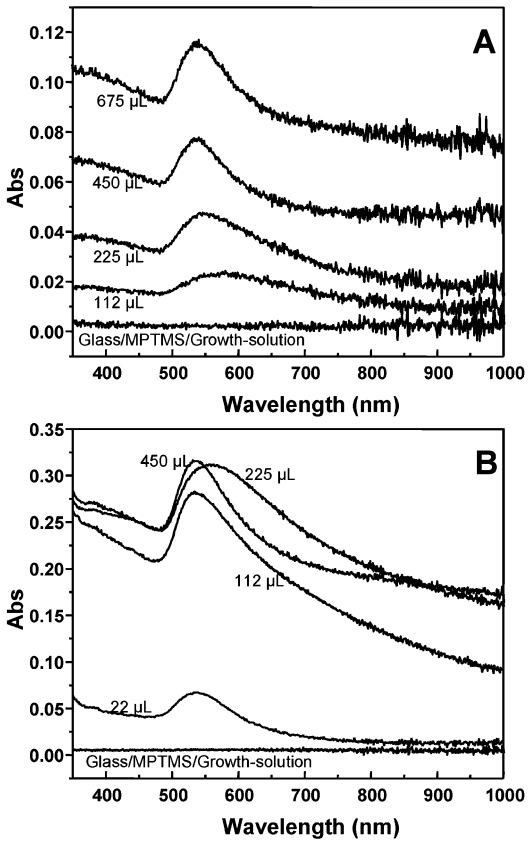

Figure 3. UV−vis spectra of glass/MPTMS/AuNP samples placed in a growth solution for (A) 1 h and (B) 21 h that contained varying amounts of $AuCl_4^-$ as indicated. The control samples where no AuNP seed was deposited on the glass (glass/MPTMS/growth solution) is also shown.

There are five possible mechanisms for the formation of the Au nanostructures on the surface: (1) Au deposition directly onto surface-attached AuNP seeds (Scheme 1), (2) AuNP catalyzed nucleation of Au to form new particles on the surface, (3) AuNP catalyzed nucleation of Au in solution and subsequent deposition on the surface, (4) spontaneous nucleation of Au directly on the glass surface, and (5) spontaneous nucleation of Au in solution and subsequent deposition on the surface. Since there is no deposition of Au on the surface without AuNP seeds present and we do not observe nucleation of Au in the growth solution with or without AuNP seeds on the surface, mechanisms 3, 4, and 5 are ruled out as contributing significantly to the observed nanostructures. Mechanism 2 may contribute to the formation of the Au nanostrucures on the surface as this has been observed previously in seed-mediated growth of Au nanoparticles in solutions with high $AuCl_4^-$/Au seed ratios and ascorbic acid as a reducing agent[48] but not with high concentrations of CTAB also in solution. Our data are most consistent with a mechanism dominated by direct deposition of Au onto surface-attached AuNP seeds, especially at low $AuCl_4^-$ concentrations.

The AFM images in Figures 1 and 2 indicate that the nanorod length and AR increase with increasing $AuCl_4^-$ concentration. This is consistent with the work of Murphy and co-workers, who previously showed that in solution, the length and AR of seed-mediated grown Au nanorods increases with increasing $AuCl_4^-$/AuNP ratio.[46−49] In our experiments, with the seed confined to the surface, the $AuCl_4^-$/AuNP ratio is 1−2 orders of magnitude larger than the highest ratio in the solution-phase experiments. The ratio in solution phase experiments ranges from 10^4 to 10^6 $AuCl_4^-$/AuNP seed, while our ratios range from 10^7 to 10^8 $AuCl_4^-$/AuNP seed, assuming a coverage of 10 AuNPs/μm^2 on a 5 cm^2 glass slide area. It is not conclusive whether the nanorod AR depends on the $AuCl_4^-$/AuNP ratio or the absolute $AuCl_4^-$ concentration for surface grown nanorods. Our general conclusion is that Au nanorod length and AR increases with increasing $AuCl_4^-$ concentration. We also conclude that a low density of AuNPs on the surface is necessary for high AR nanorods, since highly dense regions generally contain fewer and shorter Au nanorods (data not shown).

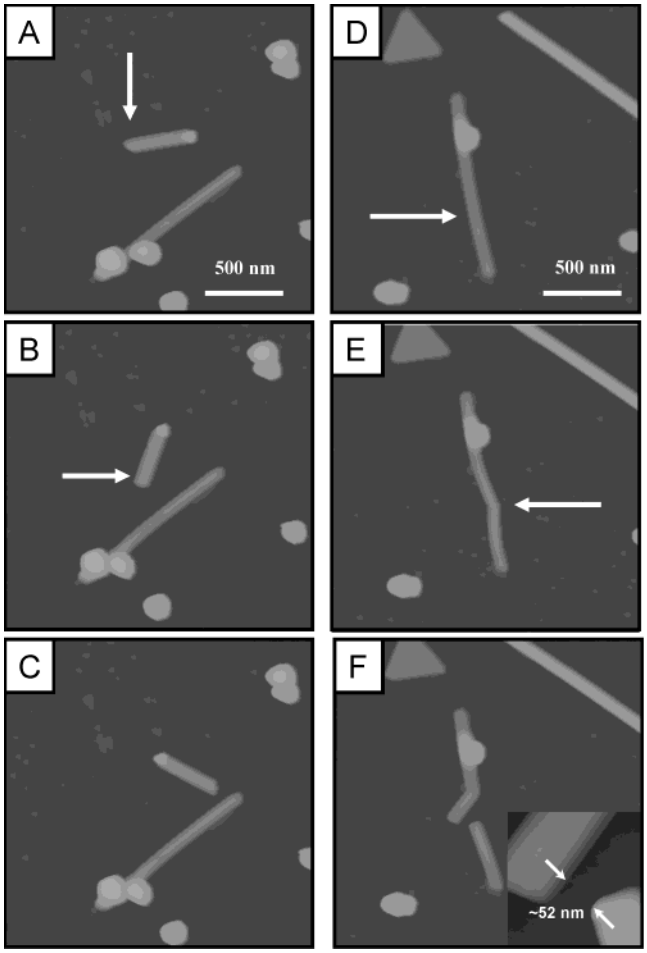

Figure 4. AFM manipulation of a 470 nm long (AR = 10) Au nanorod. The nanorod was manipulated with a tapping-mode AFM tip with the gains set to zero by offsetting in the direction shown by the arrows in frames A−C. Frames D−F show the bending and breaking of a 1.2 μm long (AR = 30) nanorod using the same manipulation conditions. The manipulation, bending, or breaking of an Au nanorod depends on the length and AR of the nanorod.

Nanorod Manipulation. Successful application of metallic nanorods will require them to be assembled onto surfaces and into larger superstructures in a controlled manner. Assembly of Au-containing nanorods has been accomplished through DNA hybridization,[60,61] biotin−streptavidin connections,[62] electric field alignment,[63] liquid crystal assembly,[64] self-assembly,[65] and scanning probe manipulation.[66] Figure 4 demonstrates the manipulation,

(60) Dujardin, E.; Hsin, L.-B.; Wang, C. R. C.; Mann, S. *Chem. Commun.* **2001**, 1264−1265.
(61) Mbindyo, J. K. N.; Reiss, B. D.; Martin, B. R.; Keating, C. D.; Natan, M. J.; Mallouk, T. E. *Adv. Mater.* **2001**, *13*, 249−254.
(62) Caswell, K. K.; Wilson, J. N.; Bunz, U. H. F.; Murphy, C. J. *J. Am. Chem. Soc.* **2003**, *125*, 13914−13915.
(63) Smith, P. A.; Nordquist, C. D.; Jackson, T. N.; Mayer, T. S.; Martin, B. R.; Mbindyo, J.; Mallouk, T. E. *Appl. Phys. Lett.* **2000**, *77*, 1399−1401.

bending, and breaking of surface-grown Au nanorods with a tapping-mode AFM tip using a procedure described previously by Hsieh et al.[66] Figure 4 shows a 470 nm long (AR = 10) Au nanorod before (frame A) and after (frame B) the nanorod was pushed by the AFM tip in the direction shown by the arrow in frame A. The nanorod was pushed by zooming in on the region at the base of the arrow, reducing the amplitude set-point by a factor of ~0.5, setting the gains to zero, and finally performing a ~1 μm offset in the direction of the arrow. Setting the gains to zero shuts off the feedback of the AFM tip and prevents it from responding to features on the surface. When it encounters the Au nanorod, the tip pushes through it instead of imaging over it. This is also demonstrated in frames B and C, resulting in another turn of the nanorod.

Interestingly, the AFM tip bent and eventually broke longer AR Au nanorods when performing a manipulation under the conditions described above. Figure 4D shows the initial image of a 1.2 μm long nanorod (AR = 30) before manipulation, and Figure 4E shows the same nanorod after it was pushed in the direction shown by the arrow in Figure 4D. The nanorod was bent near the middle in the direction of the scan. When scanning in the opposite direction under manipulation conditions, the nanorod was then broken into two shorter nanorods separated by a 52 nm gap (see Figure 4F and inset). Pushing on the nanorod twice was enough to perform a very sharp, clean break of the nanorod, presumably along one of the low index crystal planes of Au. The force required to bend and break the nanorods is unobtainable in this experiment, but this demonstration clearly shows that the mechanical properties[67] of nanorods may be probed with AFM as a function of length and AR. This is made possible by the ability to synthesize long, well-separated, high AR Au nanorods directly on surfaces.

In summary, we have demonstrated the seed-mediated growth of long, high AR Au nanorods directly on glass and studied the nanostructures by AFM and UV−vis as a function of $AuCl_4^-$ concentration and time in the growth solution. The average length and AR of the nanorods and the total amount of Au deposited on the surface increase with increasing $AuCl_4^-$ concentration for both short (1 h) and long (21 h) times in growth solution. The amount of Au deposited increases with increasing time in growth solution, but the length of nanorods was similar to the shorter times. However, the AR was significantly larger at short times, suggesting that nanorod growth occurs along the long axis within 1 h and then proceeds along the short axis at longer times under the conditions in this study. AFM is capable of manipulating, bending, or breaking Au nanorods, depending on the AR of the rod. This demonstrates the potential for controlling the placement of nanorods or studying their mechanical properties. There are many benefits for growing long, high AR nanorods that are well-separated directly on surfaces and our general approach should work for many different types of surfaces, seeds, and metals.

Acknowledgment. We acknowledge the University of Louisville for providing financial support for this research through a Competitive Enhancement Grant and the Victor A. Olorunsola Endowed Research Award for Young Scholars. We also thank one of the reviewers for suggestions regarding the linker used to attach AuNPs and the $AuCl_4^-$/AuNP seed ratio.

Supporting Information Available: UV−vis spectra of growth solutions (225 and 450 μL of $AuCl_4^-$) after glass/APTES, glass/APTES/AuNP, glass/MPTMS, and glass/MPTMS/AuNP substrates were placed in them for 1 h. UV−vis spectra of glass/APTES/AuNP and glass/MPTMS/AuNP substrates. This material is available free of charge via the Internet at http://pubs.acs.org.

LA049702I

(64) Jana, N. R.; Gearheart, L. A.; Obare, S. O.; Johnson, C. J.; Edler, K. J.; Mann, S.; Murphy, C. J. *J. Mater. Chem.* **2002**, *12*, 2909−2912.
(65) Nikoobakht, B.; Wang, Z. L.; El-Sayed, M. A. *J. Phys. Chem. B* **2000**, *104*, 8635−8640.
(66) Hsieh, S.; Meltzer, S.; Wang, C. R. C.; Requicha, A. A. G.; Thompson, M. E.; Koel, B. E. *J. Phys. Chem. B* **2002**, *106*, 231−234.
(67) Li, X.; Gao, H.; Murphy, C. J.; Caswell, K. K. *Nano Lett.* **2003**, *3*, 1495−1498.